Report Pedro Freire

Pedro Silva Freire
INESC-ID / Instituto Superior Técnico
Universidade de Lisboa, Portugal
pedro.silva.freire@tecnico.ulisboa.pt

Anderson Maciel
INESC-ID / Instituto Superior Técnico
Universidade de Lisboa, Portugal
anderson.maciel@tecnico.ulisboa.pt

João Madeiras Pereira
INESC-ID / Instituto Superior Técnico
Universidade de Lisboa, Portugal
jap@inesc-id.pt

Joaquim Jorge
INESC-ID / Instituto Superior Técnico
Universidade de Lisboa, Portugal
jorgej@acm.org

Catarina Moreira
INESC-ID / Data Science Institute
University of Technology Sydney
catarina.pintomoreira@uts.edu.au

ABSTRACT

Colon cancer remains a leading cause of cancer-related deaths, emphasizing the importance of early detection and accurate diagnostics. While colonoscopy is the gold standard, its invasiveness deters frequent, widespread use. Desktop colonography offers a less invasive alternative, and Immersive Colonography improves the efficiency of the analysis. However, colonography requires anatomical reconstruction from CTs, and liquid pockets in CT colonography often obscure the colon, necessitating dual-position scans and doubling radiation exposure. We introduce an automatic segmentation method that integrates liquid regions to eliminate the need for a second CT scan. By requiring only one CT image, this approach enhances patient safety and comfort while maintaining accurate segmentation. The developed approach uses advanced filtering and geometry-based techniques to accurately segment air and liquid pockets, ensuring continuity in colon reconstructions, we also offer a mode efficient C++ implementation. This innovation promises safer, more efficient VR colonography and improved diagnostic capabilities.

Index Terms: Colonography, Colon Segmentation, Medical Imaging

1 INTRODUCTION

Colon cancer is one of the leading causes of cancer-related deaths worldwide [19]. Early detection results in more effective treatments, underscoring the need for effective and efficient diagnostic tools. Total Colonoscopy (TC) has been the gold standard for detecting colon polyps and potentially diagnosing them as cancer [2, 16]. However, it is often perceived as invasive and uncomfortable by many patients, potentially leading to the underutilization of this critical screening method. In response, CT-colonography (CT-C) has emerged as a less invasive alternative. Unlike colonoscopy, colonography provides a non-invasive, patient-friendly procedure for examining the colon. Furthermore, recent advances allowed researchers to perform colonography in VR, with a demonstrated potential to significantly reduce the time spent on diagnostic data analysis and, consequently, the cost [17, 18].

Segmentation is a crucial step in either desktop or VR-colonography, as it allows clinicians to isolate and reconstruct the colon for detailed analysis. In CT colonography, patients often need to do a dietary preparation and take a contrast dye; usually, the bowels are inflated during the CT scan for better visualization and contrast, significantly increasing patient discomfort. In these cases, simple thresholding often results in quality results. Segmentation without bowel inflation is still a challenging problem, although recent advances allow sufficient contrast for segmentation using neural network-based methods [12].

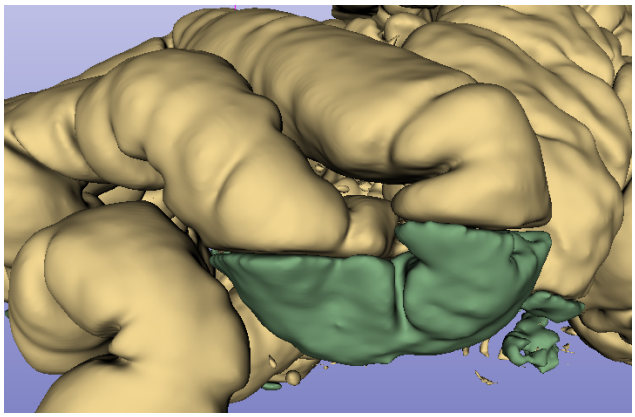

Figure 1: 3D reconstruction of the colon in yellow with the missing segment due to a liquid pocket in green

One of the key issues in colonography is minimizing patient exposure to radiation, especially when using computed tomography (CT) scans. Magnetic resonance colonography (MRC) is a promising alternative, however, MRI images typically lack the natural contrast seen in CT images, making it harder to segment the colon accurately.

For CT scans, most of the colon can be segmented using a simple contrast operation. However, many times, there are liquid pockets that obstruct or completely block the colon, as presented in Fig. 1, also, polyps in liquid pockets or at the boundary of air and liquid might not be included in the segmentation, causing false negatives. To avoid this problem, two CT scans are taken in different positions, *ventral decubitus* and *dorsal decubitus*, so that gravity displaces the liquid. Besides the extra time taken, this practice doubles the radiation exposure.

The quality of segmentation in CT colonography is essential because it affects the accuracy with which we can identify polyps. Good segmentation helps us see all the structures in the colon clearly, making it easier to spot polyps and other issues. Common pitfalls of colon segmentation, such as included feces or air bubbles, can be mistaken for polyps, leading to false positives [13].

In this work, we developed an automatic method to include the liquid in the segmentation removing the need for the second CT scan.

The main contributions of this work are as follows:

Development of a fully automated pipeline for colon segmentation, using image filtering techniques to enhance contrast, including liquid pockets, without requiring additional scans or human interaction.

Integration of air and liquid pocket segmentation into a unified reconstruction, with smoothing techniques to address boundary defects.

2 Related Work

Image segmentation is a critical task in medical imaging, enabling the identification and isolation of anatomical structures for disease detection, treatment planning, and surgical guidance. Various approaches have been developed in colon segmentation to address challenges such as liquid obstructions in virtual colonography.

Geometry-Based Methods. Traditional segmentation techniques rely on geometric properties such as shape and intensity gradients. Thresholding is a simple yet widely used method that segments high-contrast structures by converting images into binary labels. However, it struggles with low-contrast regions, artifacts, and multimodal imaging. More advanced methods, such as edge detection algorithms (e.g., Sobel and Canny filters [14]), improve segmentation by identifying intensity gradients and edge continuity. Region-growing techniques expand from seed points based on intensity similarity, as demonstrated by Franaszek et al. [4], who combined thresholding and fuzzy connectedness to segment air and liquid pockets in CT colonography. Lu et al. [10] further automated region-growing by using geodesic distances to compute the colon's centerline, eliminating the need for manual seed points. Shape detection methods, such as tubularity detection [5, 11], leverage prior knowledge of anatomical structures to improve accuracy.

Neural Network-Based Methods. Neural networks, particularly convolutional neural networks (CNNs), have revolutionized medical image segmentation by learning complex patterns from large datasets. U-Net [7] and its variants (e.g., nnU-Net [8]) are widely used due to their encoder-decoder architecture and skip connections, which capture both fine details and global context. nnU-Net, in particular, automates network configuration based on dataset properties, achieving state-of-the-art results. Large datasets, such as TotalSegmentator [20] and 8K Atlas [9, 15], have been created using semi-automatic segmentation, where radiologists refine AI-generated segmentations to improve quality.

Transformer-Based Methods. Transformers, such as Vision Transformers (ViTs) [6] and Swin Transformers [1], excel at capturing long-range dependencies and global context. However, they often underperform on smaller datasets compared to U-Nets. Hybrid architectures, such as nnFormer [21] and SAM2 [22], combine U-Net and transformer features to overcome these limitations, offering improved performance in medical imaging tasks.

While neural networks and transformers excel in general-purpose medical image segmentation, geometry-based methods remain highly effective for specific challenges, such as liquid obstructions in colon segmentation. Liquid pockets in CT colonography disrupt colon continuity, often requiring a second scan to resolve obstructions. Neural networks struggle in this context due to the lack of large, annotated datasets. Geometry-based methods, like those by Franaszek et al. [4], address these issues by leveraging spatial relationships and intensity patterns, combining thresholding and fuzzy connectedness to segment air and liquid pockets.

Building on these principles, this work develops a fully automated pipeline, eliminating the need for additional scans or manual input.

3 Method

This pipeline is designed for fully automated colon segmentation, ensuring the removal of liquid pockets that would otherwise obstruct or disrupt the colon's continuity. It follows a geometry-based approach and does not rely on deep learning models, making it robust and fully automated without the need for human intervention.

The segmentation process consists of multiple stages, as illustrated in Fig. 7:

1. **Initial segmentation:** Air-filled regions are segmented using thresholding techniques.
2. **Component filtering:** Unwanted components are removed to isolate relevant anatomical structures.
3. **Geometric boundary identification:** Flat boundary layers between air and liquid regions are detected using geometric analysis.
4. **Contrast enhancement:** Image filtering techniques are applied to enhance the contrast of high-density regions.
5. **Liquid pocket segmentation:** A region-growing algorithm is used to segment liquid pockets based on a defined intensity threshold.
6. **Integration and refinement:** The segmented air and liquid regions are merged, followed by Gaussian smoothing to produce the final segmentation output.

The code to our implementation of the pipeline is available on Github[1] there is also a slower but equivalent presentation in python.Github[2]

The next sections provide detailed explanations of each step in the pipeline.

3.1 Thresholding for air pockets.

In this initial step, we use a straightforward thresholding operation on the unmodified Ct image with an upper bound of $-800HU$ to reliably identify all air-filled segments, including unwanted structures that must be removed.

To filter out these unwanted elements we employ a simple yet effective heuristics that doesn´t require any human interaction. Firstly, a connected components algorithm is applied with components smaller than a predefined size threshold being discarded.

We begin by removing the top and bottom slices of the image. This step is crucial because, in our observations, the lungs are truncated at the edges of these slices. As a result, both the lungs and the surrounding bed and background layers are eliminated. However, there is an exception: if a component contains very few voxels, we retain it. This is important in cases where the tube used for colon inflation appears in the bottom slice and connects to the colon component.

After this first step, the result is that the air parts of the colon are segmented; this can be only one component or many if the liquid pockets break the colon continuity.

3.2 Boundary Layer Detection

To effectively detect and merge the liquid pockets with the air pockets, it is crucial to identify the boundary regions between them. To achieve this, we first locate flat, downward-facing surfaces within the air pockets. These initial detections are then refined using the Sobel filter to enhance the clarity of the boundaries.

To generate the labels, we employ the Sobel operator. To speed up the process, we only compute the Sobel gradient for voxels that belong to the air segmentation. First, we calculate the Sobel filter along the Y-axis, and only if the gradient direction matches the expected boundary, do we proceed to calculate the Sobel gradients

[1] GitHub repository: https://github.com/PedroSFreire/CppSegPipeline
[2] GitHub repository: https://github.com/PedroSFreire/GeometricalColonSeg

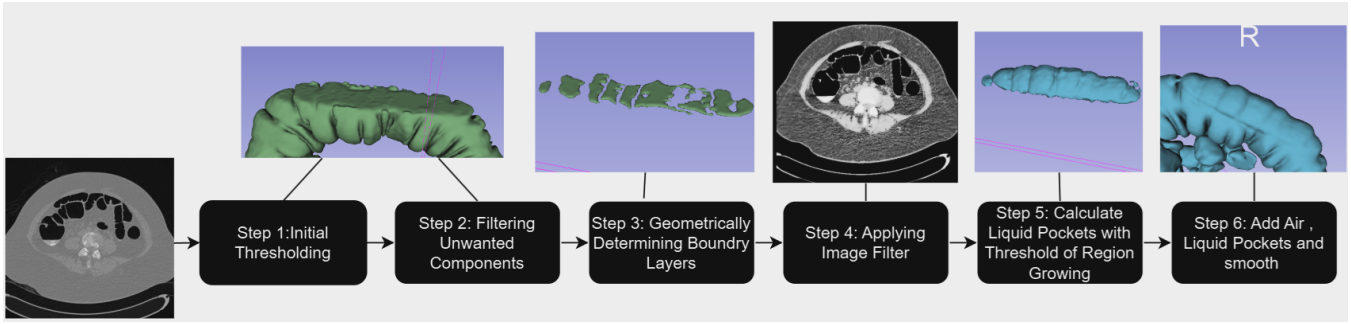

Figure 2: Flowchart of the linear pipeline, with images for the segmented air and liquid pockets, the detected boundary layers, and the final result.

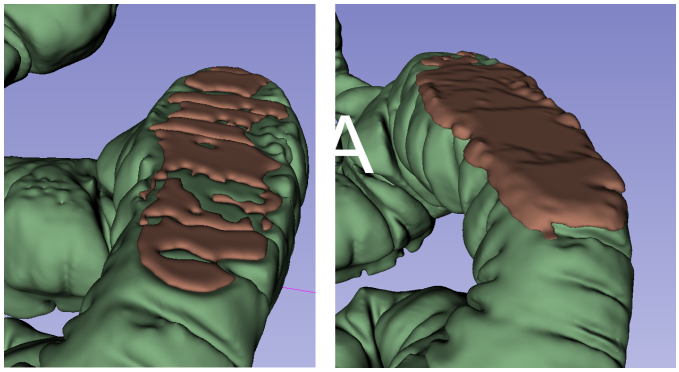

Figure 3: Reconstruction of air pockets of the colon. On the left with the flat label before expansion. On the right with the flat label region growing.

in the X and Z directions. This selective approach significantly accelerates the process compared to applying the Sobel filter across the entire image.

Next, using the Sobel values, we filter the image based on the gradient similarity to the target surface normal, and group the results into connected components. A size threshold is then applied to remove small, irrelevant surfaces, leaving only the significant components, which we refer to as "flat labels."

At this stage, the flat labels are still imperfect. After segmenting the liquid pockets, any labels that intersect with a liquid pocket undergo a region-growing process, which is guided by the Y-gradient direction from the Sobel filter. Labels that do not intersect with liquid pockets are discarded. To fill any gaps in the segmentation, we add any unassigned voxel located between a label voxel and a liquid pocket voxel to the label, ensuring continuity and minimizing segmentation holes. The result can be seen in Fig. 3.

3.3 Image Filtering

Segmenting liquid pockets presents significant challenges. The contrast liquid often settles at the bottom of the pockets, making it difficult to achieve consistent segmentation(Figs. 4-right and 5-right). Additionally, low contrast between liquid and surrounding dense organs can cause leakage into those regions. Simple thresholding may also inadvertently include bones and other dense tissues, further complicating the segmentation process.

To address this issue, we apply filters to enhance contrast before segmenting the liquid pockets. The process begins with intensity clamping, which reduces noise and isolates relevant tissue types by restricting the intensity values to a meaningful range. Next, histogram equalization enhances contrast within the liquid pockets, making them more distinguishable. Finally, an anisotropic filter is

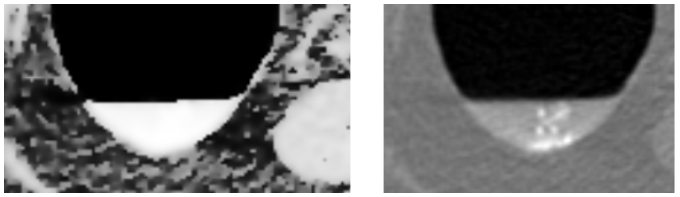

Figure 4: On the left, the contrast-enhanced ct on the right, the original. We can see the settled contrast is mostly gone.

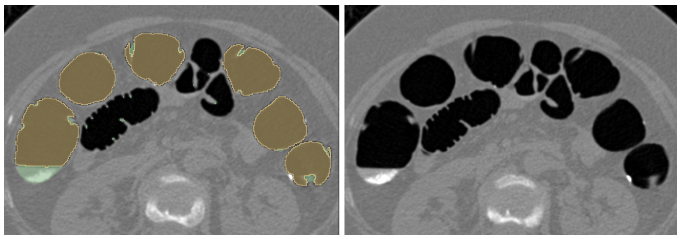

Figure 5: On the left, a segmentation of the colon is shown by a mask overlay highlighting air pockets in yellow and liquid pockets in green. This was achieved using our method. The image on the right is the unprocessed CT scan, where the heterogeneity of the contrast within the liquid pockets is more evident.

applied to reduce noise while preserving edges, ensuring a clearer and more accurate segmentation. An example of the combined result of the filter can be seen in Fig.4.

3.4 Segmentation of Pockets Using Thresholding

To segment the liquid pockets we observe promising results when applying simple threshold segmentation with a lower bound of 200HU to the enhanced images to isolate the liquid pockets. However, several issues persist, many of which can be addressed with further refinement.

The primary challenge is the inclusion of unwanted structures such as bones, liquid pockets in the small bowel, and other soft tissues. To mitigate this, we leverage the previously identified flat labels from the air-filled regions of the colon.

The refinement process begins by running a connected-components algorithm. Components intersecting with the previously calculated flat labels are retained, ensuring only relevant structures are included. Additionally, the detected flat labels are incorporated the segmentation to assist in defining the air-liquid boundary more accurately.

3.5 Intersection of Components and Boundary Region Growing

In the final step of the pipeline, we have already calculated three separate images: one representing the air pockets, another representing the liquid pockets, and the third representing the boundary regions. The goal of this step is to identify the labels that intersect both the air pockets and the liquid pockets.

Since the boundary regions are already located on the borders of the air pockets, we begin by checking for labels that intersect with a liquid pocket. If such an intersection is found, the corresponding air and liquid pockets are considered valid and included in the final segmentation image.

After confirming that the label is valid, we perform region growing on the label. This process helps refine the label and ensures the accurate representation of the combined air and liquid regions.

4 C++ IMPROVED PIPELINE FLOW

The pipeline is divided into three main stages:

1. **Stage 1 – Air and Flat Label Detection:** This stage involves the segmentation of air-filled regions (air labels) and the identification of flat boundary regions (flat labels), followed by component-wise filtering to remove irrelevant components.

2. **Stage 2 – Liquid Pocket Segmentation:** The base image is filtered to enhance the contrast of liquid regions. These enhanced regions are then segmented into liquid pockets and filtered by connected components. This stage also includes an *anisotropic diffusion* step, which is executed on the **GPU** to improve performance due to its highly parallel nature.

3. **Stage 3 – Label Intersection and Final Region Growing:** The results from the first two stages are intersected to determine valid components. Flat labels that intersect both air and liquid regions are retained and refined via region growing to complete the final segmentation.

Stages 1 and 2 are **asynchronous** and can be executed in parallel. Synchronization is only required before entering Stage 3 to combine the results.

Additionally, `OpenMP` (`omp.h`) is used throughout the pipeline to parallelize computational loops, effectively leveraging **multi-core CPUs** alongside the **GPU** to achieve high performance.

5 EXPERIMENTAL SETUP

The dataset used for evaluation is extracted from the Colon CT dataset [3]. This dataset contains CT scans of the colon, but no ground truth segmentation data is available, which limits the ability to provide quantitative metrics. Consequently, our evaluation is based on a qualitative visual inspection of the segmentation results.

The pipeline was implemented both in Python which operates sequentially and C++ with a multicore aproach that also uses the GPU for higher performance. The experiments were conducted on a laptop with an AMD Ryzen 7 7840HS processor, an NVIDIA GeForce RTX 4060 GPU, and 32 GB of RAM.

For validation, three CT volumes from the dataset were processed and analyzed. The evaluation focused on the framework's ability to segment air and liquid pockets, handle liquid obstructions, and maintain the continuity of the colon in 3D reconstructions. The results were qualitatively assessed by visual inspection.

[3] available at: `www.cancerimagingarchive.net/access-data/`

6 RESULTS

Fig. 5 shows a 2D slice of the CT scan, where the air pockets in the colon are correctly segmented. The 3D reconstruction highlights the continuity of the segmented colon, with air pockets in yellow and liquid pockets in green. The method successfully integrates liquid obstructions into the segmentation, addressing one of the key challenges in colon segmentation without requiring a second CT scan.

Fig. 6 provides additional visual evidence of the segmentation quality, showing both internal and external views of the colon. The method effectively handles low-contrast regions and complex boundaries, ensuring liquid pockets are accurately segmented and integrated with air-filled regions.

Each CT scan has a resolution of 512×512×625, and the runtime for processing a single scan in the python pipeline takes 20 to 30 minutes while the C++ implementation takes less than a minute(40 to 50 seconds).

Our experiments resulted in the following key observations:
Segmentation Accuracy: The method successfully segments air and liquid pockets, even in challenging cases with low contrast or complex boundaries. The integration of liquid obstructions into the overall segmentation is visually accurate. As this work is ongoing, we still have not run specific metrics.
Continuity: The 3D reconstructions demonstrate good continuity of the segmented colon, with minimal artifacts or disconnected components.
Limitations: Some minor artifacts and over-smoothing at air-liquid boundaries were observed, which could be addressed in future refinements.

These results demonstrate the potential of the developed approach in segmenting air and liquid pockets while maintaining the continuity of the colon. However, some limitations remain, which highlight areas for future improvement.

7 DISCUSSION

The developed approach demonstrates strong potential for automated colon segmentation, particularly in its ability to accurately segment air and liquid pockets while maintaining the continuity of the colon in 3D reconstructions. These results highlight the effectiveness of the approach in addressing key challenges in colon segmentation, such as handling liquid obstructions and ensuring smooth transitions between segmented regions. While there are areas for further refinement, the current implementation provides a solid foundation for future advancements. Below, we discuss the strengths of the method and opportunities for improvement in three key areas: segmentation quality, computational performance, and algorithm robustness.

Segmentation Quality. The method accurately calculates air and liquid pockets, even in challenging cases with low contrast or complex boundaries. The integration of liquid obstructions into the overall segmentation is a notable strength, as it eliminates the need for additional scans or manual intervention. The 3D reconstructions demonstrate good continuity, with minimal artifacts or disconnected components, critical for clinical applications such as virtual colonoscopy. However, some minor artifacts were observed, such as low-quality seams at air-liquid boundaries and occasional smoothing artifacts. These issues are relatively minor and do not detract significantly from the overall segmentation quality but could be further refined to enhance the method's precision. Future work could incorporate advanced boundary refinement techniques, such as horizontal region expansion methods [4], to improve the delineation of air-liquid interfaces.

Computational Performance. The current C++ implementation demonstrates high performance, making it well-suited for batch processing of CT scans in research environments or for AI training

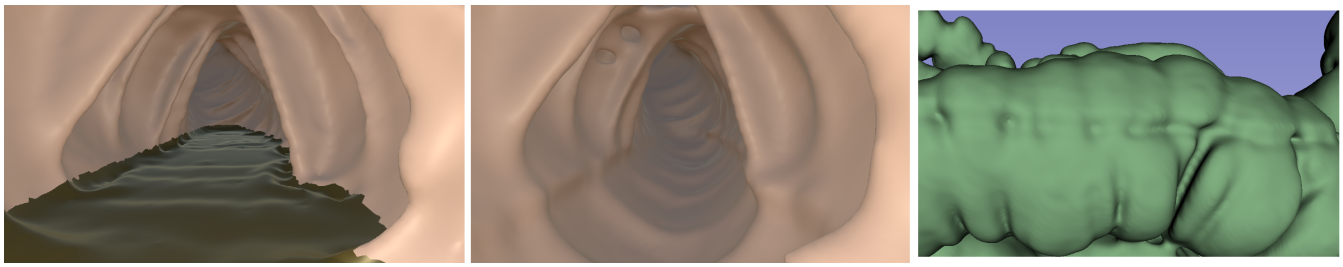

Figure 6: The reconstruction as viewed in VR. Left: The result of a simple air-tissue threshold-based segmentation, which fails to include the liquid pockets. Center: The 3D reconstruction produced by our segmentation algorithm merging the air and liquid pockets. Right: The external view of our reconstruction shows light artifacts at the seams of the liquid pocket.

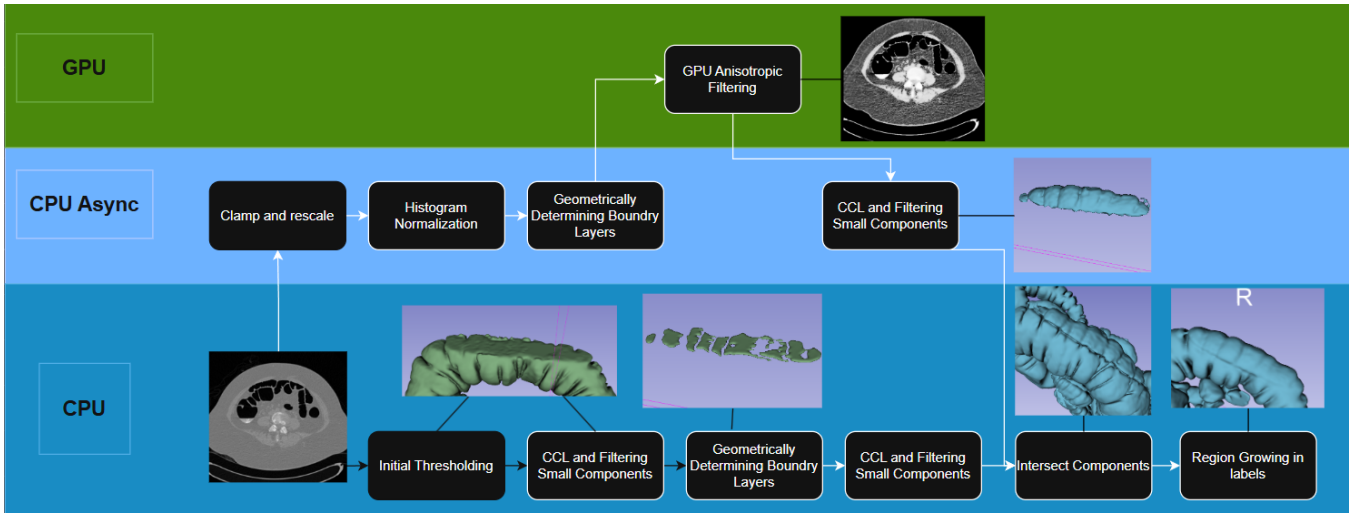

Figure 7: Optimized pipeline making use of multicore and GPU.

purposes. Its short execution time also highlights its potential for practical application in clinical settings.

Algorithm Robustness. The algorithm's robustness is another key strength, as it performs well across various cases, including those with low contrast or complex anatomical structures. Using contrast enhancement filters and region-growing techniques ensures that air and liquid pockets are accurately segmented in most scenarios. However, there is room for further refinement to make the method even more adaptable to diverse datasets and challenging conditions. For example, while effective, using fixed thresholds and basic intensity-based filters may not generalize optimally to all cases. Incorporating more sophisticated expansion techniques, such as those based on Gaussian or cosine similarity metrics, could improve the accuracy of region growth and reduce the occurrence of expansion leaks.

8 Conclusion

This project resulted in the development of a high-performance, fully automated segmentation pipeline for CT colonography. By addressing the common challenge of liquid pockets obstructing segmentation, our solution eliminates the need for multiple scans, thereby reducing patient discomfort and radiation exposure. The integration of GPU-based anisotropic filtering and CPU-based multicore parallelism ensures fast execution, making the tool suitable for batch processing in research contexts or potential clinical applications.

A key achievement of this work was the successful expansion and refinement of a previously existing solution [3]. The new implementation not only automates the entire segmentation process but also effectively includes liquid pockets in the final segmentation, significantly improving anatomical completeness and diagnostic reliability.

Throughout the development of this project, I significantly expanded my knowledge of both Python and C++, with a strong emphasis on advanced C++ techniques. In particular, I gained valuable experience in optimizing performance using multicore processing with OpenMP and implementing GPU acceleration. These skills not only improved the efficiency of the final pipeline but also deepened my understanding of high-performance computing in medical imaging applications.

9 Future Work

The asynchronous thread completes significantly faster than the main thread. This idle time presents an opportunity to enhance segmentation quality without impacting overall performance. For instance, an early liquid pocket expansion step could be added here to better capture challenging liquid pockets, ensuring higher-quality inclusion in the final segmentation. Additionally, this spare time could be used to apply a more comprehensive filter stack, further improving the definition of liquid pockets all at no extra performance cost.

Acknowledgments

The work reported in this article was partially supported under the auspices of the UNESCO Chair on AI & VR by national funds through Fundação para a Ciência e a Tecnologia with references DOI:10.54499/ UIDB/50021/2020,

DOI:10.54499/DL57/2016/CP1368/CT0002 and 2022.09212.PTDC (XAVIER project).

REFERENCES

[1] H. Cao, Y. Wang, J. Chen, D. Jiang, X. Zhang, Q. Tian, and M. Wang. Swin-unet: Unet-like pure transformer for medical image segmentation. In *European conference on computer vision*, pp. 205–218. Springer, 2022.

[2] V. K. Dik, L. M. Moons, and P. D. Siersema. Endoscopic innovations to increase the adenoma detection rate during colonoscopy. *World journal of gastroenterology: WJG*, 20(9):2200, 2014.

[3] S. F Paulo, N. Figueiredo, J. Jorge, and D. Lopes. 3d reconstruction of ct colonography models for vr/ar applications using free software tools, 09 2018. doi: 10.13140/RG.2.2.26893.18405

[4] M. Franaszek, R. M. Summers, P. J. Pickhardt, and J. R. Choi. Hybrid segmentation of colon filled with air and opacified fluid for ct colonography. *IEEE transactions on medical imaging*, 25(3):358–368, 2006.

[5] C. Hennersperger, M. Baust, P. Waelkens, A. Karamalis, S.-A. Ahmadi, and N. Navab. Multi-scale tubular structure detection in ultrasound imaging. *IEEE Transactions on Medical Imaging*, 34(1):13–26, 2014.

[6] E. U. Henry, O. Emebob, and C. A. Omonhinmin. Vision transformers in medical imaging: A review. *arXiv preprint arXiv:2211.10043*, 2022.

[7] Z. Huang, H. Wang, Z. Deng, J. Ye, Y. Su, H. Sun, J. Junjun He, Y. Gu, L. Gu, S. Zhang, et al. Stu-net: Scalable and transferable medical image segmentation models empowered by large-scale supervised pre-training [internet]. arxiv; 2023 [cited 2023 may 5].

[8] F. Isensee, J. Petersen, A. Klein, D. Zimmerer, P. F. Jaeger, S. Kohl, J. Wasserthal, G. Koehler, T. Norajitra, S. Wirkert, and K. H. Maier-Hein. nnu-net: Self-adapting framework for u-net-based medical image segmentation, 2018.

[9] W. Li, C. Qu, X. Chen, P. R. Bassi, Y. Shi, Y. Lai, Q. Yu, H. Xue, Y. Chen, X. Lin, et al. Abdomenatlas: A large-scale, detailed-annotated, & multi-center dataset for efficient transfer learning and open algorithmic benchmarking. *Medical Image Analysis*, 97:103285, 2024.

[10] L. Lu, D. Zhang, L. Li, and J. Zhao. Fully automated colon segmentation for the computation of complete colon centerline in virtual colonoscopy. *IEEE Transactions on Biomedical Engineering*, 59(4):996–1004, 2012. doi: 10.1109/TBME.2011.2182051

[11] B. Orellana, E. Monclús, P. Brunet, I. Navazo, Á. Bendezú, and F. Azpiroz. A scalable approach to t2-mri colon segmentation. *Medical image analysis*, 63:101697, 2020.

[12] B. Orellana, E. Monclús, I. Navazo, Bendezú, C. Malagelada, and F. Azpiroz. End to end colonic content assessment: Colonmetry application. *Diagnostics*, 13(5), 2023. doi: 10.3390/diagnostics13050910

[13] P. J. Pickhardt and D. H. Kim. Ct colonography: pitfalls in interpretation. *Radiologic Clinics*, 51(1):69–88, 2013.

[14] J. H. Pujar, P. S. Gurjal, K. S. Kunnur, et al. Medical image segmentation based on vigorous smoothing and edge detection ideology. *International Journal of Electrical and Computer Engineering*, 4(8):1143–1149, 2010.

[15] C. Qu, T. Zhang, H. Qiao, Y. Tang, A. L. Yuille, Z. Zhou, et al. Abdomenatlas-8k: Annotating 8,000 ct volumes for multi-organ segmentation in three weeks. *Advances in Neural Information Processing Systems*, 36, 2024.

[16] D. K. Rex, P. S. Schoenfeld, J. Cohen, I. M. Pike, D. G. Adler, M. B. Fennerty, J. G. Lieb, W. G. Park, M. K. Rizk, M. S. Sawhney, et al. Quality indicators for colonoscopy. *Gastrointestinal endoscopy*, 81(1):31–53, 2015.

[17] J. Serras, A. Duchowski, I. Nobre, C. Moreira, A. Maciel, and J. Jorge. Immersive virtual colonography viewer for colon growths diagnosis: Design and think aloud study. *Multimodal Technologies and Interaction*, 8(5), 2024. doi: 10.3390/mti8050040

[18] J. Serras, A. Maciel, S. Paulo, A. Duchowski, R. Kopper, C. Moreira, and J. Jorge. Development of an immersive virtual colonoscopy viewer for colon growths diagnosis. In *2023 IEEE Conference on Virtual Reality and 3D User Interfaces Abstracts and Workshops (VRW)*, pp. 152–155, 2023. doi: 10.1109/VRW58643.2023.00038

[19] R. L. Siegel, N. S. Wagle, A. Cercek, R. A. Smith, and A. Jemal. Colorectal cancer statistics, 2023. *CA: a cancer journal for clinicians*, 73(3):233–254, 2023.

[20] J. Wasserthal, H.-C. Breit, M. T. Meyer, M. Pradella, D. Hinck, A. W. Sauter, T. Heye, D. T. Boll, J. Cyriac, S. Yang, et al. Totalsegmentator: robust segmentation of 104 anatomic structures in ct images. *Radiology: Artificial Intelligence*, 5(5), 2023.

[21] H.-Y. Zhou, J. Guo, Y. Zhang, X. Han, L. Yu, L. Wang, and Y. Yu. nnformer: Volumetric medical image segmentation via a 3d transformer. *IEEE Transactions on Image Processing*, 2023.

[22] J. Zhu, Y. Qi, and J. Wu. Medical sam 2: Segment medical images as video via segment anything model 2. *arXiv preprint arXiv:2408.00874*, 2024.